Article

Journal of the Brazilian Chemical Society

https://dx.doi.org/10.21577/0103-5053.20240082

J. Braz. Chem. Soc. **2025**, *36*, 1, e-20240082, 1-8

In vitro Metabolism and Cytotoxicity of Parthenolide: The Complete Identification of the Major Oxidative Product and the Evaluation of Trypanocidal and Leishmanicidal Activities

Maíra R. S. Silvério,[a] Daniel Roberto Callejon,[b] João M. Batista Jr.,[c] Thalita B. Riul,[d] Anderson Rodrigo M. de Oliveira[e] and Norberto P. Lopes *,[a]

[a]*Núcleo de Pesquisa de Produtos Naturais e Sintéticos (NPPNS), Departamento de Ciências BioMoleculares, Faculdade de Ciências Farmacêuticas de Ribeirão Preto, Universidade de São Paulo, 14040-903 Ribeirão Preto-SP, Brazil*

[b]*Yosen Nanotechnology, 14056-680 Ribeirão Preto-SP, Brazil*

[c]*Instituto de Ciência e Tecnologia, Universidade Federal de São Paulo, 12247-014 São José dos Campos-SP, Brazil*

[d]*Faculdade de Ciências Farmacêuticas, Alimentos e Nutrição, Universidade Federal de Mato Grosso do Sul, 79070-900 Campo Grande-MS, Brazil*

[e]*Departamento de Química, Faculdade de Filosofia, Ciências e Letras de Ribeirão Preto, Universidade de São Paulo, 14040-901 Ribeirão Preto-SP, Brazil*

Parthenolide (PTN) is a secondary metabolite of the plant *Tanacetum parthenium* (L.) Schulz Bip. and is considered the chemical marker of this species. This sesquiterpene lactone (germacrene skeleton) has been described as responsible for the biological activity of the leaf extract. In addition, several studies in the literature have demonstrated its antiparasitic and antineoplastic activity. However, there is a need for knowledge of other safety parameters, such as pharmacokinetic, pharmacodynamic and toxicity evaluations. Therefore, in this investigation, the *in vitro* metabolism of parthenolide was performed with rat liver microsomes and biomimetic metabolism (such as cytochrome P-450 system) using organometallic catalysts. The biomimetic procedure was validated since the major compound of biomimetic oxidative reaction with *meta*-chloroperbenzoic acid catalyzed by metalloporphyrin 5,10,15,20-tetrakis(pentafluorophenyl)-porphyrin iron(III) chloride was also observed with rat liver microsomes. Previous chemoenzymatic synthesis studies of PTN afforded the same epoxide formation, this major oxidative compound was isolated and fully characterized as (1*R*,10*R*)-epoxyparthenolide based on experimental and theoretical calculations of infrared (IR) and vibrational circular dichroism (VCD) data at the B3PW91/6-311G. Furthermore, for the first time, this metabolite was evaluated for trypanocidal and leishmanicidal activity. The mean inhibitory concentration (IC_{50}) values were lower for PTN than its metabolite and showed significant cytotoxic effects for both parasites. This finding holds promise for addressing neglected diseases.

Keywords: parthenolide, (1*R*,10*R*)-epoxyparthenolide, biomimetic oxidation, liver microsomal metabolism, trypanocidal, leishmanicidal

Introduction

Parthenolide (PTN) (**1**) (Figure 1) is a sesquiterpene lactone (germacrolide moiety) considered as the chemical marker of *Tanacetum parthenium* (L.) Schulz Bip. species and described as responsible for the biological activity of the leaf extract.[1] The standardized extract is presented in the Brazilian market as an herbal medicine for headache prevention (simplified registration at the Agência Nacional de Vigilância Sanitária (Anvisa) Instrução Normativa No. 02 de 13 de maio de 2014).[2] The popular use of this species is for menstrual disorders, auxiliary in the treatment of arthritis, stomach disorders and fever.[1]

Furthermore, multiple studies in the literature[3-6] have shown that PTN exhibits antiparasitic and antineoplastic activities. However, limited research has been conducted to evaluate critical properties of PTN, including

*e-mail: npelopes@fcfrp.usp.br
Editor handled this article: Hector Henrique F. Koolen (Associate)

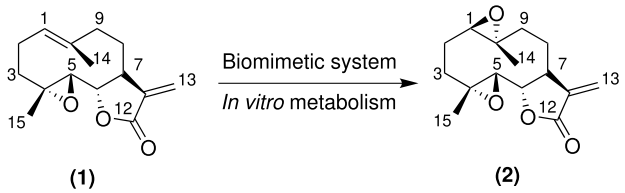

Figure 1. Oxidative reaction of parthenolide after *in vitro* oxidative metabolism. The highest yield was through metaboloporphyrins with a 40% rate of metabolite formation.

pharmacokinetics, pharmacodynamics, and toxicity.[7-9] Other studies on the metabolism of PTN have shown that this sesquiterpenic lactone has a short half-life (1.38 h) and a low bioavailability (7.78%) when administered orally in a pharmacokinetic study carried out in rats[10] and that it was not detectable in human plasma in a phase I study in which *Tanacetum parthenium* extract was administered orally.[8] A vital step in the toxicological assessment of an active substance involves characterizing its metabolism, which can be achieved through *in vitro* assays, such as biomimetic oxidative models and rat liver microsomes.

The biomimetic oxidative model usually uses a porphyrin-based catalytic agent, which has similarity to cytochrome P-450 (CYP450) enzymes, and an oxidizing agent.[11-14] The metalloporphyrin 5,10,15,20-tetrakis(pentafluorophenyl)-porphyrin iron(III) chloride (FeTFPPCl) can catalyze a wide range of CYP450-mediated reactions, including epoxidation, aliphatic and aromatic hydroxylation, and the oxidation of heteroatoms.[13,15] *meta*-Chloroperbenzoic acid (MCPBA) is a commonly used oxidant in metalloporphyrin-based biomimetic systems, especially for epoxidation reactions.[15,16] The rat liver microsomal and pig cecum model have been extensively used for the *in vitro* metabolism of several natural products.[17-19] *In vitro* systems have important advantages over *in vivo* systems, such as higher yields of oxidized metabolites, reproducibility of reactions, reduced animal use, and lower cost.[12]

Therefore, the aim of this work was to carry out the analysis of PTN after *in vitro* biomimetic reactions (such as CYP450 system using organometallic catalysts) and microsomal metabolism. In addition, the trypanocidal and leishmanicidal activities of PTN and its main compound isolated from the oxidative biomimetic system were evaluated.

Results and Discussion

The biomimetic metabolism of PTN, catalyzed by the metalloporphyrin FeTFPPCl, was carried out in the presence of MCPBA. The mass spectrum of PTN samples after *in vitro* metabolism by oxidative biomimetic model showed a major metabolite with *m/z* 265 $[M + H]^+$ (Figure S7, Supplementary Information (SI) section). This major oxidative product was isolated by semi-preparative high performance liquid chromatography-diode array detector (HPLC-DAD) and identified using the techniques of ^1H and ^{13}C spectroscopy nuclear magnetic resonance (NMR) and electrospray ionization high-resolution mass spectrometry (ESI-HRMS). The absolute configurations of PTN and its oxidative product were determined by vibrational circular dichroism (VCD) spectroscopy and density functional theory (DFT) calculations. Therefore, the putative metabolite was fully identified as (1*R*,10*R*)-epoxyparthenolide (**2**) (Figure 1).

The *in vitro* metabolism performed by rat liver microsomes and analyzed by liquid chromatography-electrospray ionization-mass spectrometry (LC-ESI-MS) revealed that the oxidative product **2** (Figure 1) was the sole metabolite produced by the *in vitro* biological model.

The mean inhibitory concentration (IC_{50}), cell viability and the similarity index obtained from the cytotoxic assay using promastigotes forms of *Leishmania amazonensis* (*L. amazonensis*), tripomastigotes of *Trypanosoma cruzi* (*T. cruzi*) and a murine macrophage-like cell line are shown in Table 1. Through these *in vitro* assays, it was possible to evaluate that PTN and the oxidized product exhibited significant cytotoxic activity in both cellular forms of the parasites and in mammals. The cytotoxic effects of both PTN and (1*R*,10*R*)-epoxyparthenolide were more selective for the parasitic strains of *T. cruzi*, as demonstrated by low

Table 1. Cell viability in the presence of PTN and the putative metabolite (1*R*,10*R*)-epoxyparthenolide (**2**)

	Leishmania amazonensis (IC_{50}) / (μmol L^{-1})	*Trypanossoma cruzi* (IC_{50}) / (μmol L^{-1})	Cell line J774 (CC_{50})	SI[a]	SI[b]
PTN	16.47	2.42	14.84	0.90	6.13
Metabolite 2	43.03	4.13	16.05	0.37	3.88
Amphotericin B	1.64	–	–	–	–
Benznidazole	–	14.7	–	–	–

[a]SI related to *L. amazonensis*; [b]SI related to *T. cruzi*. PTN: parthenolide; IC_{50}: half-maximal inhibitory concentration; CC_{50}: half-maximal cytotoxic concentration; SI: selective index: CC_{50} drug/IC_{50} drug.

IC_{50} value and show high selectivity for this parasite, as previously reported by other natural products.[20,21] It is interesting to note that compound **2** was less cytotoxic than PTN. Furthermore, the IC_{50} for the trypomastigote forms of *T. cruzi* was lower for both compounds than that of benznidazole.

The mass spectrum of the isolated product of oxidative biomimetic metabolism shows the addition (on the protonated ion) of 16 u in the molecular mass of PTN, suggesting the addition of only one oxygen atom in the molecule and the fragmentation showed some expected open ring fragmentations. The ^{1}H and ^{13}C NMR analysis suggests that the oxygen atom has been inserted into the double bond of the 1,10-position. The mass spectrum is shown in Figure S1, and the NMR spectra are shown in Figures S2 and S3, SI section. In more details, the identification by NMR, the ^{1}H (Figure S2), ^{13}C NMR (Figure S3), DEPT-135 (Figure S8) spectra and contour maps of heteronuclear single quantum coherence spectroscopy (HSQC, Figure S9) and heteronuclear multiple bond correlation (HMBC, Figure S10) were analyzed, the data of which are described in Table 2 and the spectra and contour maps are included at the Supplementary Information section. Analysis of the ^{13}C and ^{1}H NMR spectra revealed the presence of 15 carbons and 20 hydrogens, respectively.

In the ^{13}C NMR spectrum, as well as in the HSQC contour map, four signals of non-hydrogenated carbons were observed, including a carbonyl group at δ 168.8, suggestive of the ester function, a carbon at δ 138.8, suggestive of unsaturated carbon (sp2) and two carbons at δ 60.7 and 60.5, suggesting connection to the electronegative atom; five signals from methylene carbons, one from the alkene function (δ_H/δ_C 6.36; 5.63/121.3); four signals of methine carbons, three of which are unshielded (δ_H/δ_C 3.95/81.8; 2.93/64.6 and 2.86/63.7), suggesting connection to the electronegative atom and two signals of methyl carbons (δ_H/δ_C 1.40/17.1 and 1.35/17.5). ^{1}H NMR experiments allowed the identification of two vinyl hydrogens at δ 6.35 (1H, d, *J* 3.6 Hz) and δ 5.63 (1H, d, *J* 3.2 Hz); four unshielded methine hydrogens at δ 3.95 (1H, tl, *J* 8.9 Hz), δ 2.93 (1H, d, *J* 8.9 Hz); δ 2.86 (1H, dd, *J* 1.3 and 11.0 Hz) and δ 2.74 (1H, m); four methylene hydrogens and two methyl hydrogens. Detailed assignments of the hydrogen and carbon signals were sequentially assigned by combinations of two-dimensional HSQC and HMBC techniques. Connectivity was established by correlations in the HMBC contour map, represented in Figure S11 (SI section). The methylene hydrogens in position 9 showed a correlation with the methine carbons in positions 1 and 7 and the methyl carbon in position 14, as well as the methylene carbon in position 8. The methine hydrogen in position 1 showed a correlation with the methylene carbon in position 2 and the methyl hydrogen in position 6 with the methyl carbon in position 5. Furthermore, the methyl hydrogens in position 15 showed a correlation with the methin carbons in position 5 and methylene carbon in position 3. Take together all NMR data and comparison with the previous data of PTN[6-22] confirmed the epoxide formation. The mass spectrometry (MS) data revealed a similar behavior for sesquiterpene lactones, including a delicate balance between protonated molecule and sodium coordination in MS.[23] ESI-HRMS was calculated based on sodium molecule showing the signal at *m/z* 287.1265 (theoretical mass 287.1254 corresponding to $C_{15}H_{20}O_4Na$; 3.83 error). Finally, the MS/MS of the protonated molecule at *m/z* 265 showed, as expected, two water eliminations (ion at *m/z* 247 and 229),[24] as well as the expected opening of the five-membered lactone ring affording ion at *m/z* 237[25] followed by two sequential water eliminations at *m/z* 219 and *m/z* 201. Take together all NMR and MS data confirm the relative configuration of the metabolite **2**.

The relative configuration of PTN was previously determined by X-ray crystallography. Therefore, two

Table 2. ^{1}H (400 MHz, $CDCl_3$) and ^{13}C NMR data obtained for the isolated oxidized product

1*R*,10*R*-Epoxyparthenolide (**2**)		
Position	δ_H (mult., *J*) / ppm	δ_C C-type / ppm
1	2.86 (dd, 1.3, 11.0)	63.9
2	2.19 (m)	24.26
	1.52 (m)	
3	2.28 (m)	35.3
	1.42 (m)	
4	–	60.7
5	2.91 (d, 8.9)	64.7
6	3.95 (tl, 8.8)	81.9
7	2.74 (m)	47.9
8	2.22 (m)	26.2
	1.62 (m)	
9	2.48 (dd, 7.6, 14.2)	40.3
	1.24 (tl, 13.3)	
10	–	60.8
11	–	138.9
12	–	168.9
13	6.35 (d, 3.6)	121.5
	5.63 (d, 3.2)	
14	1.40 (s)	17.2
15	1.35 (s)	17.6

mult: multiplicities.

absolute configurations were possible, (4*R*,5*R*,6*S*,7*S*)-(**1a**) and (4*S*,5*S*,6*R*,7*R*)-(**1b**). The excellent agreement between experimental and calculated infrared (IR) and VCD data at the B3PW91/6-311G(d,p)[26] level confirms that the absolute configuration of PTN is 4*R*,5*R*,6*S*,7*S* (Figure 2). Once the absolute configuration of PTN was assigned, the next step was to determine the absolute stereochemistry of the additional epoxide at C-1 and C-10 in **2**. For this purpose, the IR and VCD spectra of both diastereoisomers, i.e., (4*R*,5*R*,6*S*,7*S*,1*R*,10*R*)-(**2a**) and (4*R*,5*R*,6*S*,7*S*,1*S*,10*S*)-(**2b**), were also calculated and compared to experiment. An overall better agreement between experimental and calculated data was observed for (4*R*,5*R*,6*S*,7*S*,1*R*,10*R*)-(**2a**) at the B3PW91/6-311G(d,p) level (Figure 2). The most important differences were observed for the bands at 1000-1100 cm^{-1}, which arise from C–C stretching involving most of the molecular framework as well as CH_3 deformation modes. Therefore, the absolute configuration of **2** was assigned as 4*R*,5*R*,6*S*,7*S*,1*R*,10*R*. Thus, the putative metabolite was identified as (1*R*,10*R*)-epoxyparthenolide (Figure 1).

To establish a correlation between the oxidation reaction and the biological processes of drug metabolism, PTN was subjected to *in vitro* metabolism using rat liver microsomes. The unique metabolite produced in the *in vitro* biological model was the same major metabolite obtained and isolated from the biomimetic oxidation reaction (Figure 1). The mass spectra of the products are shown in Figure S4, SI section. As previously described, PTN metabolism studies showed a short half-life (1.38 h) and a low bioavailability (7.78%) in rats[10] and that it was not detectable in human plasma.[11] On the other hand, the (1*R*,10*R*)-epoxyparthenolide was also chemoenzymatic synthesis applying variants of *Bacillus megaterium*, but no absolute stereochemistry was defined.[9]

In addition, cytotoxicity was evaluated with PTN and (1*R*,10*R*)-epoxyparthenolide in *L. amazonensis* and *T. cruzi* parasites. The results showed that both compounds induced significant cytotoxic effects in intracellular parasite forms and in mammalian cells. *T. cruzi* was the parasite that showed the greatest reduction in viability. Some studies have shown that PTN has cytotoxic effect on different forms of the parasites. Rabito *et al.*[27] showed that the extract fraction from the aerial parts of *Tanacetum parthenium* (L.) Schultz-Bip induced significant

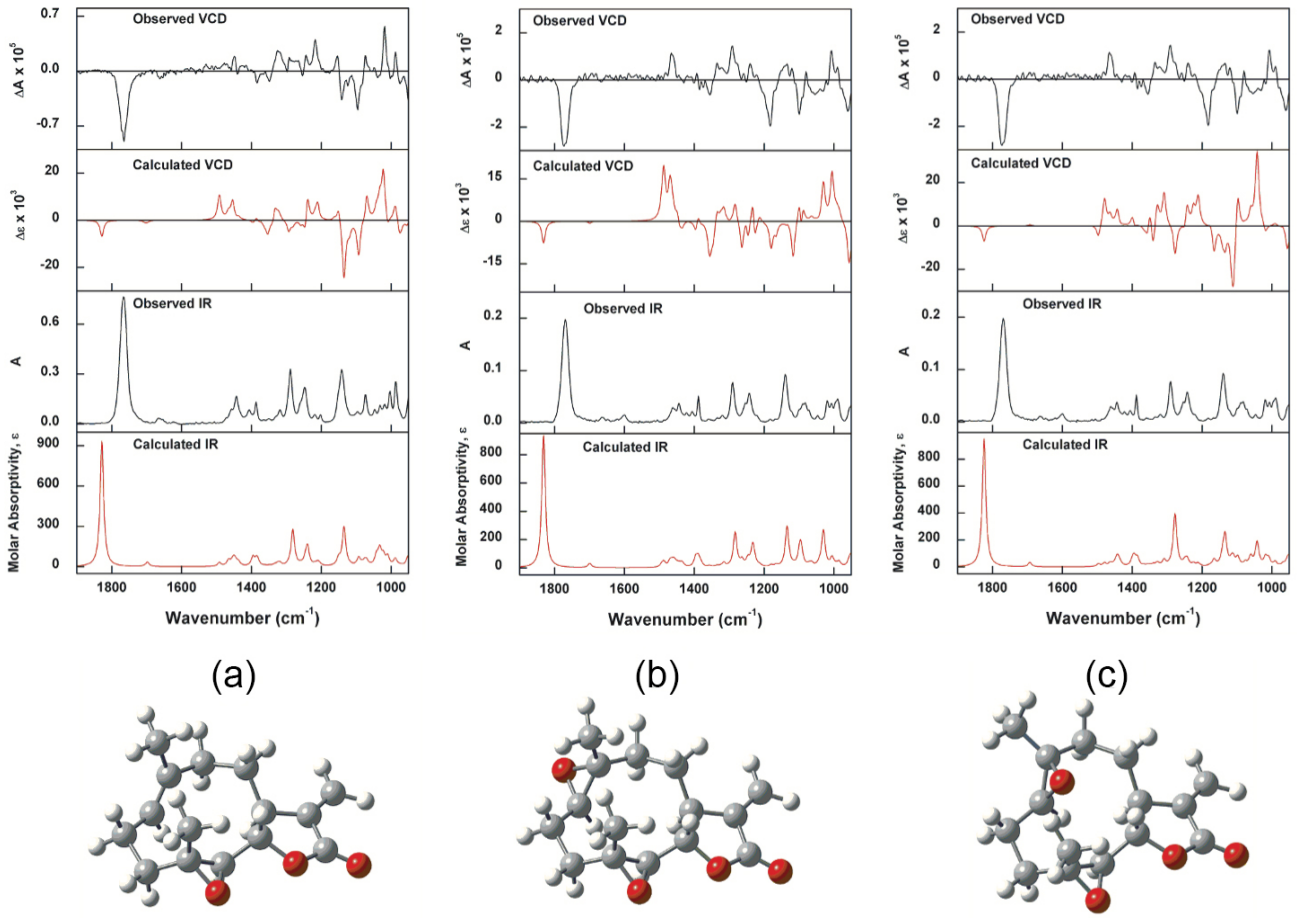

Figure 2. Observed and calculated (B3PW91/6-311G(d,p)) IR and VCD spectra and optimized structure of the lowest-energy conformer for (a) (4*R*,5*R*,6*S*,7*S*)-(**1**), (b) (4*R*,5*R*,6*S*,7*S*,1*R*,10*R*)-(**2**), and (c) (4*R*,5*R*,6*S*,7*S*,1*S*,10*S*)-(**2**).

antileishmanial activity on *Leishmania amazonensis*. Tiuman *et al*.[28] demonstrated PTN to have significant activity against the promastigote form of *L. amazonensis* and Pelizzaro-Rocha *et al*.[29] verified that PTN had a significant cytotoxic effect on *T. cruzi*. The effect of PTN on *T. cruzi* was associated with morphological changes, changes that significantly alter the shape form of the parasite and consequently loss of the plasma membrane integrity.

The IC_{50} value of PTN and its metabolite obtained from *in vitro* assays was lower than that of benznidazole, the current standard of care for the treatment of Chagas disease.[30] On the other hand, the presence of PTN and its metabolite in *L. amazonensis* promastigote form showed that PTN induced more cytotoxicity than its putative metabolite. These results suggest that metabolically induced structural changes on the PTN molecule may reduce its leishmanicidal activity but not its trypanocidal activity. In conclusion, FeTFPPCl catalyzed oxidation of PTN resulted in the formation of a predominant putative metabolite, which was the same product observed during *in vitro* metabolism by rat liver microsomes, confirming its suitability as a chemical model for drug metabolism. This oxidized product from the biomimetic system was, for the first time, fully characterized as (1*R*,10*R*)-epoxyparthenolide and submitted for trypanocidal and leishmanicidal activity. In addition, the cytotoxicity results suggest that this product has a similar effect to that of parthenolide for trypanocidal activity (reduction of cell viability of *T. cruzi* trypomastigote form). However, the putative metabolite was less effective in reducing cell viability of *L. amazonensis* promastigote forms. The literature data on metabolism and the results of this study reinforce the need to evaluate this metabolite in further pharmacological and toxicological studies of PTN in order to achieve a safer and more effective herbal medicine.

Conclusions

The parthenolide reaction, when scaled with FeTFPPCl and MCPBA, led to the identification of a putative major metabolite: (1*R*,10*R*)-epoxy-parthenolide. This characterization was achieved using techniques such as NMR, HRMS-ESI, and VCD, allowing the absolute stereochemistry confirmation. In the context of microsomal *in vitro* metabolism, only one metabolite was detected. Interestingly, this suggests that the same product is formed during biomimetic oxidation and is also as previously produced in chemoenzymatic synthesis. In terms of biological activity, the cytotoxicity assay demonstrated that the metabolite (1*R*,10*R*)-epoxy-parthenolide exhibits a similar effect to parthenolide in a tested model of trypanocidal activity. Notably, both compounds showed greater efficacy than the positive control benznidazole. However, this effect was not observed in the leishmanicidal assay. These findings underscore the importance of evaluating both compounds in pharmacological and toxicological models, with the aim of potential application in Chagas disease protocols.

Experimental

Chemicals and materials

FeTFPPCl, MCPBA (purity 74.5%, titration), parthenolide (purity 99%, high-performance liquid chromatography (HPLC) degree) and deuterated chloroform which were purchased from Sigma-Aldrich (Saint Louis, USA). Acetonitrile was HPLC grade (J.T. Baker, Phillipsburg, USA). Type I ultrapure water was obtained from Milli-Q (Millipore brand purification system, Darmstadt, Germany).

Biomimetic oxidation

The reaction was carried out at room temperature, in the absence of air and light, in a screw-capped glass vessel equipped with a magnetic stirring rod. A catalyst FeTFPPCl (0.12 mmol L^{-1}), the substrate (3.6 mmol L^{-1} PTN) and the oxidant (3.6 mmol L^{-1} MCPBA) were dissolved in acetonitrile to a total volume of 2.0 mL (total of 30 vessels). Control samples were prepared (*i*) in the absence of catalyst and (*ii*) in the absence of catalyst and oxidant.

After the reaction time (24 h), the solvent was evaporated in an air atmosphere and, immediately before injection into the chromatographic system, the fraction was solubilized in 1 mL of acetonitrile and filtered through a 0.45 µm PTFE (polytetrafluoroethylene) membrane.

The isolation was performed in a semi-preparative HPLC-DAD equipment (Shimadzu Corp., Kyoto, Japan, two pumps LC 6AD, diode array detector SPD-M20A, communicator CBM-20A and an integration software LCSolutions) with preparative Shimadzu ODS column (250 mm × 20 mm, 5 µm particle size). A gradient program was used with the mobile phase combining ultrapure water (solvent A) and acetonitrile (solvent B) as follows: 20% B (0-10 min), 48% B (22-42 min), 100% B (46-52 min). The flow rate was 9.0 mL min^{-1} and the injection volume was 1.0 mL. The collected fractions containing the putative metabolite were pooled and lyophilized.

Characterization of putative metabolites

Nuclear magnetic resonance (NMR, Bruker-Advance DRX 400, Karlsruhe, Germany) of ^1H was in 400 MHz

and ^{13}C was in 100 MHz. Approximately 10 mg of the compound were dissolved in $CDCl_3$ for analysis.

High-resolution electrospray ionization mass spectrometry (ESI-HRMS, micrOTOF-Q II, Bruker Daltonics, Karlsruhe, Germany), in positive mode, with time-of-flight (TOF) analyzer. Approximately 1 mg of the compound was dissolved in acetonitrile:water with 0.1% formic acid (v/v, 1:1) for direct infusion analysis (50-1000 *m/z*).

The IR and VCD spectra of compounds **1** and **2** were recorded with a BioTools Dual-PEM Chiral*IR*-2X FT-VCD (Jupiter, USA) spectrometer with a resolution of 4 cm^{-1} and a collection time of 7 h. The optimum retardation of the two ZnSe photoelastic modulators (PEMs) was set at 1400 cm^{-1}. Minor instrumental baseline offsets were eliminated from the final VCD spectra by subtraction of the VCD spectra of compounds **1** and **2** from that of the solvent under the same conditions. The IR and VCD spectra were recorded in $CDCl_3$ solutions (3.8 mg of **1** and 2.5 mg of **2** in 150 µL of $CDCl_3$ in a 100 µm path length BaF_2 cell). All density functional theory (DFT) calculations were performed at 298 K in the gas phase using Gaussian 09 software (Revision A.02).[31] Calculations were performed for the arbitrarily chosen (4*R*,5*R*,6*S*,7*S*)-**1a** as well as (4*R*,5*R*,6*S*,7*S*,1*R*,10*R*)-**2a** and (4*R*,5*R*,6*S*,7*S*,1*S*,10*S*)-**2b**. All conformational searches were performed at the molecular mechanics level of theory with the Monte Carlo algorithm using the MM^+ force field included in the HyperChem 8.0.10 software package.[32] A single conformer was identified for compound (**1**), and for both diastereoisomers of compound (**2**). The lowest energy conformer for each configuration was then geometry optimized at the B3PW91/6-311G(d,p) level. IR and VCD spectra were constructed using dipole and rotational strengths from Gaussian, which were calculated at the B3PW91/6-311G(d,p) level and converted to molar absorptivities (mol^{-1} cm^{-1}). Each spectrum was plotted as a sum of Lorentzian bands with half-widths at half-maximum of 6 cm^{-1}. The calculated wavenumbers were multiplied by a scaling factor of 0.98 and the spectra were plotted using Origin 8 software.[33]

Microsomal *in vitro* metabolism procedure

The nicotinamide adenine dinucleotide phosphate (NADPH) regenerating system was added to test tube: 50 µL nicotinamide adenine dinucleotide (NAD) + hydrogen (H) (2.5 mmol L^{-1}), 50 µL glucose-6-phosphate (5 mmol L^{-1}) and 25 µL glucose-6-phosphate dehydrogenase (0.5 units); 50 µL rat liver microsomal preparation (1.0 mg mL^{-1} microsomal protein), pre-warmed at 37 °C for 5 min; 10 µL of the substrate PTN (7.0 µg mL^{-1}) and 315 µL of phosphate buffer (250 mmol L^{-1}). The reaction was then initiated by the addition of the rat liver microsomal preparation and incubated for 60 min (37 °C) using a shaking water bath (Dubnoff-SL157, Solab, Piracicaba, Brazil). The reaction was terminated by the addition of ethyl acetate (1.0 mL). To extract the PTN and its metabolites from the reaction medium, the sample was shaken for 10 min at 1200 rpm (Vibrax VXR, IKA, Wilmington, United States) and centrifuged for 12 min at 1792 ×g at 6 °C (Hitachi CF16RXII, Himac, Tokyo, Japan). The supernatant was collected, transferred to another vial and dried under a gentle stream of nitrogen. Control samples were prepared (*i*) in the absence of the NADPH-regenerating system and (*ii*) in the absence of rat liver microsomes. The samples were solubilized in acetonitrile and injected into an HPLC-DAD instrument (Shimadzu Corp., Kyoto, Japan - two pumps LC 20AD, diode array detector SPD-M20A, oven CTO-20A, auto injector SIL-20AHT, communicator CBM-20A) coupled to an ion trap mass analyzer with electrospray ionization (amaZon, Bruker, Karlsruhe, Germany). The software used was HyStar for analysis and DataAnalysis for processing. The column used was a Shimadzu (Kyoto, Japan) Shim-pack XR-ODS (100 mm × 3 mm, 2.2 µm particle size) and a gradient program was used with the mobile phase combining ultrapure water with 0.1% of formic acid (solvent A) and acetonitrile with 0.1% of formic acid (solvent B) as follows: 21% B (0 min), 32% B (5-17 min), 48% B (20-30 min). The column was maintained at 40 °C, the flow rate was 0.3 mL min^{-1} and the injection volume was 4.0 µL.

Cytotoxic assay

The cytotoxic assay was performed using promastigotes forms of *L. amazonensis*, trypomastigotes forms of *T. cruzi* and the murine macrophage-like cell line J744.[34,35] Cell death controls were treated with amphotericin B for leishmanicidal activity and benznidazole for trypanocidal activity.

To evaluate the cytotoxicity induced by PTN and its putative metabolite treatment generated in the parasite *L. amazonensis* and in the cell line J774, the MTT assay (3-(4,5-dimethylthiazol-2-yl)-2,5-diphenyltetrazolium bromide) was used. The promastigote forms of *L. amazonensis* (1×10^6 cells *per* well) were cultured in 96-well plates and incubated with different concentrations in dimethyl sulfoxide (DMSO) of parthenolide and its metabolite (0.78, 1.56, 3.125, 6.25, 12.5, 25 50, 100 µmol L^{-1}) for 24 h. After incubation, the plate was centrifuged at 900 ×g for 15 min, the supernatants were removed, and 200 µL MTT solution (5 mg mL^{-1}) were added

to each well. After 3 h of incubation, the culture plate was centrifuged again (900 ×g for 15 min), the supernatants were removed, and 200 µL of DMSO was added to solubilize the blue formazan crystals. The evaluation of the cytotoxicity of parthenolide and its metabolite in the J774 cell line was also performed by the MTT assay, using a similar approach as for the promastigote forms. Absorbance was measured using a spectrophotometer (SpectraMax Plus, Molecular Devices, San Jose, USA) at 492 nm results were expressed as percentage (%) of cells able to reduce MTT and/or formazan producers relative to the viability control.

The resazurin assay was used to evaluate the effect of PTN and its metabolite on *T. cruzi.* Trypomastigote forms of *T. cruzi* (1×10^6 *per* well) were added to 96-well plates and treated with different concentrations of parthenolide and its metabolite (0.78, 1.56, 3.125, 6.25, 12.5, 25, 50, 100 µmol L^{-1}) for 24 h in culture medium in complete Roswell Park Memorial Institute (RPMI) medium at 37 °C with 5% CO_2. At the end of the treatment period, 5 µL resazurin (1 mg mL^{-1}) was added to each well, and the plates were maintained at 37 °C with 5 % CO_2 for 18 h. Absorbance was measured using a spectrophotometer (SpectraMax Plus, Molecular Devices, San Jose, USA) at 570 and 600 nm for the viability calculation.

(1*R*,10*R*)-Epoxiparthenolide (**2**)

White powder, NMR data see Table 2. ESI-HRMS observed mass at *m/z* 287.1265 for $[\mathbf{2} + Na]^+$ calcd. 287.1254; 3.83 error. For VCD and IR see Figure 2.

Supplementary Information

Supplementary information (the detailed information on (1*R*,10*R*)-epoxyparthenolide characterization, NMR spectra and mass spectra of the *in vitro* metabolism assay) is available free of charge at http://jbcs.sbq.org.br as PDF file.

Acknowledgments

The authors thank FINEP, FAPESP, CAPES, and CNPq for financial support. The authors thank the São Paulo Research Foundation (FAPESP, grant numbers: 2014/25222-9; 2016/07597-0; 2018/07534-4), the Conselho Nacional de Desenvolvimento Científico e Tecnológico (CNPq), and the Coordenação de Aperfeiçoamento de Pessoal de Nível Superior - Brasil (CAPES) - Finance Code 001 for financial support and for granting research fellowships. This research was also supported by resources supplied by the Centre for Scientific Computing (NCC/GridUNESP) of São Paulo State University (UNESP).

Author Contributions

The project involved collaborative efforts from multiple authors. Maíra R. S. Silvério and Norberto P. Lopes conceptualized the study. Maíra R. S. Silvério handled data curation related to isolation and metabolism, while João M. Batista Jr. focused on stereochemistry. Daniel R. Callejon contributed to data curation for biological assays. João M. Batista Jr. conducted formal analysis specifically related to stereochemistry, and Thalita B. Riul performed formal analysis for biological assays. Anderson R. M. de Oliveira was involved in the investigation of metabolism. Norberto P. Lopes oversaw general aspects, including project administration and resource management. Maíra R. S. Silvério and Norberto P. Lopes jointly wrote the original draft, and all authors collaborated on writing, reviewing, and editing.

References

1. Preeti, A.; Pushpa, S.; Sakshi, S.; Jyoti, A.; *Int. Res. J. Pharm*. **2012**, *3*, 65. [Crossref]
2. Ministério da Saúde, Agência Nacional de Vigilância Sanitária (ANVISA); Instrução Normativa No. 02 de 13 de maio de 2014, Publica a "*Lista de Medicamentos Fitoterápicos de Registro Simplificado*" e a "*Lista de ProdutosTtradicionais Fitoterápicos de Registro Simplificado*"; Anvisa: Brasília, 2014. [Link] accessed in May 2024
3. Kim, S. L.; Liu, Y. C.; Ran, P. J.; Seo, S. Y.; Kim, S. H.; Kim, E. H.; Lee, S. O.; Lee, S. T.; Kim, D. G.; Kim, S. W.; *Int. J. Oncol*. **2015**, *46*, 1121. [Crossref]
4. Popiolek-Barczyk, K.; Kolosowska, N.; Piotrowska, A.; Makuch, W.; Rojewska, E.; Jurga, A. M.; Pilat, D.; Mika, J.; *Neural Plast.* **2015**, *2015*, 676473. [Crossref]
5. Nam, Y. J.; Lee, D. H.; Lee; Lee, M. S.; Lee, C. S.; *Arch. Pharmacol*. **2015**, *388*, 921. [Crossref]
6. Tiuman, T. S.; Ueda-Nakamura, T.; Alonso, A.; Nakamura, C. V.; *BMC Microbiol.* **2014**, *14*, 152. [Crossref]
7. Curry III, E. A.; Murry, D. J.; Yoder, C.; Fife, K.; Armstrong, V.; Nakshatri, H.; O'Connell, M.; Sweeney, C. J.; *Invest. New Drugs* **2004**, *22*, 299. [Crossref]
8. Zhao, A. Q.; Zhao, J. H.; Zhang, S.; Pan, Y. Y., Huo, X. L.; *J. Pharm. Biom. Anal.* **2016**, *119*, 99. [Crossref]
9. Kolev, J. N.; O´Dwyer, K. M.; Jordan, C. T.; Fasan, R.; *ACS Chem. Biol.* **2014**, *9*, 164. [Crossref]
10. Santos, M. D.; Lopes, N. P.; *Quim. Nova* **2008**, *31*, 767. [Crossref]
11. Niehues, M.; Barros V. P.; Emery, F. S.; Dias-Baruffi, M.; Assis, M.; Lopes, N. P.; *Eur. J. Med. Chem*. **2012**, *54*, 804. [Crossref]
12. Bernadou, J.; Meunier, B.; *Adv. Synth. Catal.* **2004**, *346*, 171. [Crossref]

13. Costas, M.; *Coord. Chem. Rev*. **2011**, *255*, 2912. [Crossref]
14. Clososki, G. C.; Soldi, R. A.; Silva, R. M.; Guaratini, T.; Lopes, J. N. C.; Pereira, P. R. R.; Lopes, J. L. C.; Santos, T.; Martins, R. B.; Costa, C. S.; Carvalho, A. N.; Silva, L. P.; Arruda, E.; Lopes, N. P.; *J. Braz. Chem. Soc*. **2020**, *31*, 1552. [Crossref]
15. Meunier, B.; Bernadou, J.; *Top. Catal.* **2002**, *21*, 47. [Crossref]
16. Lohmann, W.; Karst, U.; *Anal. Bioanal. Chem*. **2008**, *391*, 79. [Crossref]
17. Thomazzi, S. M.; Moreira, F. L.; Turatti, I. C. C.; Paula e Souza, J. N.; Andrade, L. N.; Silva, D. B.; Oliveira, A. R. M.; De Souza, D. P.; Lopes, N. P.; *Planta Med. Lett*. **2015**, *2*, e61. [Crossref]
18. Ferreira, L. S.; Callejon, D. R.; Engemann, A.; Cramer, B.; Humpf, H. U.; de Barros, V. P.; Assis, M. D.; da Silva, D. B.; Albuquerque, S.; Okano, L. T.; Kato, M. J.; Lopes, N. P.; *Planta Med*. **2012**, *78*, 1939. [Crossref]
19. Labib, S.; Hummel, S.; Richling, E.; Humpf, H. U.; Schreier, P.; *Mol. Nutr. Food Res*. **2006**, *50*, 78. [Crossref]
20. Barreiro-Costa, O.; Lozano, C. Q.; Muñoz, E.; Rojas-Silva, P.; Medeiros, A.; Comini, M. A.; Heredia-Moya, J.; *Biomedicines* **2022**, *10*, 1913. [Crossref]
21. García-Huertas, P.; Olmo, F.; Sánchez-Moreno, M.; Dominguez, J.; Chahboun, R.; Triana-Chávez, O.; *Exp. Parasitol*. **2018**, *189*, 34. [Crossref]
22. Gören, N.; Tahtasakal, E.; *Phytochemistry* **1997**, *45*, 107. [Crossref]
23. Crotti A. E. M.; Lopes, J. L. C.; Lopes, N. P.; *J. Mass Spectrom*. **2005**, *40*, 1030. [Crossref]
24. Lopes, N. P.; Stark, C. B. W.; Gates, P. J.; Staunton, J.; *Analyst* **2002**, *127*, 503. [Crossref]
25. Crotti, A. E. M.; Fonseca, T.; Hong, H.; Staunton, J.; Galembeck, S. E.; Lopes, N. P.; Gates, P. J.; *Int. J. Mass Spectrom*. **2004**, *232*, 271. [Crossref]
26. Runge E.; Gross, E. K. U.; *Phys. Rev. Lett*. **1984**, *52*, 997. [Crossref]
27. Rabito, M. F.; Britta, E. A.; Pelegrini, B. L.; Almeida, M. B.; Nakamura, C. V.; Ferreira, I. C.; *Exp. Parasitol*. **2014**, *143*, 18. [Crossref]
28. Tiuman, T. S.; Ueda-Nakamura, T., Cortez, D. A. G.; Filho, B. P. D.; Morgado-Díaz, J. A.; Souza, W.; Nakamura, C. V.; *Antimicrob. Agents Chemother* **2005**, *49*, 176. [Crossref]
29. Pelizzaro-Rocha, K. J.; Tiuman, T. S.; Izumi, E.; Ueda-Nakamura, T.; Dias Filho, B. P.; Nakamura, C. V.; *Phytomedicine* **2010**, *18*, 36. [Crossref]
30. Molina, I.; Perin, L.; Aviles, A. S.; Vieira, P. M. A.; Fonseca, K. S.; Cunha, L. M.; Carneiro, C. M.; *Acta Trop*. **2020**, *201*, 105218. [Crossref]
31. Frisch, M. J.; Trucks, G. W.; Schlegel, H. B.; Scuseria, G. E.; Robb, M. A.; Cheeseman, J. R.; Scalmani, G.; Barone, V.; Mennucci, B.; Petersson, G. A.; Nakatsuji, H.; Caricato, M.; Li, X.; Hratchian, H. P.; Izmaylov, A. F.; Bloino, J.; Zheng, G.; Sonnenberg, J. L.; Hada, M.; Ehara, M.; Toyota, K.; Fukuda, R.; Hasegawa, J.; Ishida, M.; Nakajima, T.; Honda, Y.; Kitao, O.; Nakai, H.; Vreven, T.; Montgomery, Jr., J. A.; Peralta, J. E.; Ogliaro, F.; Bearpark, M.; Heyd, J. J.; Brothers, E.; Kudin, K. N.; Staroverov, V. N.; Kobayashi, R.; Normand, J.; Raghavachari, K.; Rendell, A.; Burant, J. C.; Iyengar, S. S.; Tomasi, J.; Cossi, M.; Rega, N.; Millam, J. M.; Klene, M.; Knox, J. E.; Cross, J. B.; Bakken, V.; Adamo, C.; Jaramillo, J.; Gomperts, R.; Stratmann, R. E.; Yazyev, O.; Austin, A. J.; Cammi, R.; Pomelli, C.; Ochterski, J. W.; Martin, R. L.; Morokuma, K.; Zakrzewski, V. G.; Voth, G. A.; Salvador, P.; Dannenberg, J. J.; Dapprich, S.; Daniels, A. D.; Farkas, Ö.; Foresman, J. B.; Ortiz, J. V.; Cioslowski, J.; Fox, D. J.; *Gaussian 09*, Revision A.02, Gaussian Inc., Wallingford CT, 2009.
32. *HyperChem*, 8.0.10; Makolab, Florida, USA, 2007.
33. *Origin Pro* 8; OriginLab, Northampton, USA, 2009.
34. Rolon, M.; Vega, C.; Escario, J. A.; Gomez-Barrio, A.; *Parasitol. Res.* **2006**, *99*, 103. [Crossref]
35. Perrot, S.; Dutertre-Catella, H.; Martin, C.; Rat, P.; Warnet, J. M.; *Toxicol. Sci*. **2003**, *72*, 122. [Crossref]

Submitted: February 8, 2024
Published online: May 22, 2024